

Continuous summer export of nitrogen-rich organic matter from the Greenland Ice Sheet inferred by ultrahigh resolution mass spectrometry

Emily C. Lawson, Maya P. Bhatia, Jemma L. Wadham, Elizabeth B. Kujawinski

E. C. Lawson*†, Bristol Glaciology Centre, School of Geographical Sciences, University
Road, Bristol, BS8 1SS, U.K (emily.lawson@nottingham.ac.uk)

M. P. Bhatia, Department of Microbiology and Immunology, University of British Columbia,
Vancouver, BC, V6T 1Z3, Canada (mayab3@mail.ubc.ca)

J. L. Wadham, Bristol Glaciology Centre, School of Geographical Sciences, University of
Bristol, University Road, Bristol, BS8 1SS, U.K (j.l.wadham@bristol.ac.uk)

E. B. Kujawinski, Department of Marine Chemistry and Geochemistry, Woods Hole
Oceanographic Institution, Woods Hole, MA, 02543, USA (ekujawinski@whoi.edu)

1 ABSTRACT

2 Runoff from glaciers and ice sheets has been acknowledged as a potential source of
3 bioavailable dissolved organic matter (DOM) to downstream ecosystems. This source may
4 become increasingly significant as glacial melt rates increase in response to future climate
5 change. Recent work has identified significant concentrations of bioavailable carbon and iron
6 in Greenland Ice Sheet (GrIS) runoff. The flux characteristics and export of N-rich DOM are
7 poorly understood. Here, we employed electrospray ionization (ESI) coupled to Fourier
8 transform ion cyclotron resonance mass spectrometry (FT-ICR MS) to determine the
9 elemental compositions of DOM molecules in supraglacial water and subglacial runoff from
10 a large GrIS outlet glacier. We provide the first detailed temporal analysis of the molecular
11 composition of DOM exported over a full melt season. We find that DOM pools in
12 supraglacial and subglacial runoff are compositionally diverse and that N-rich material is
13 continuously exported throughout the melt season as the snowline retreats further inland.
14 Identification of protein-like compounds and a high proportion of N-rich DOM, accounting
15 for 27-41% of the DOM molecules identified by ESI FT-ICR MS, may suggest a microbial
16 provenance and high bioavailability of glacially-exported DOM to downstream microbial
17 communities.

18 INTRODUCTION AND RATIONALE

19 Glacial runoff has recently been acknowledged as an important source of nutrients to
20 downstream coastal and marine ecosystems¹⁻⁴. Total nutrient fluxes from glaciers are
21 predominantly controlled by freshwater fluxes and the physico-chemical and microbiological
22 cycling of nutrients at the glacier surface^{5, 6} and bed^{7, 8}. Here we focus on the Greenland Ice
23 Sheet (GrIS), where outlet glaciers discharge *c.* 1000 Gt yr⁻¹ freshwater runoff to the
24 neighboring oceans⁹. Freshwater fluxes from the GrIS into the North Atlantic are increasing
25 at a rate of $16.9 \pm 1.8 \text{ km}^3 \text{ yr}^{-1}$ ⁹, which may enhance the net terrestrial export of nutrients
26 from the ice sheet. This has the potential to impact primary productivity at local¹⁰ and
27 regional scales¹¹ and may affect fjord and marine microbial food webs¹². Recent work
28 suggests that meltwater discharged from the GrIS may export significant quantities of
29 potentially bioavailable dissolved organic matter (DOM)^{2, 4} and iron^{3, 13} to the coastal oceans.
30 Glacially-exported DOM contains a high proportion of protein-like compounds^{1, 14, 15},
31 suggesting the potential export of bioavailable dissolved organic nitrogen (DON). Several
32 studies have estimated the annual DON yield in glacial runoff¹⁶⁻¹⁸ and suggested a
33 microbial^{19, 20} or aerosol provenance²¹ for DON compounds. However, the abundance and
34 character of the nitrogen-rich compounds in the DOM are still not well known. High N:C
35 elemental ratios (≥ 0.27 ; determined by electrospray ionization (ESI) coupled to Fourier
36 transform ion cyclotron resonance mass spectrometry (FT-ICR MS) following C₁₈ DOM
37 extraction) in supraglacial samples from a small (5 km²) western GrIS outlet glacier suggest
38 that nitrogen-containing compounds are an important component of DOM²⁰. However, this
39 research has yet to be extended over an entire melt season and to large GrIS catchments.

40

41 DOM exported from glaciers reflects OM provenance (allochthonous or autochthonous),
42 age and source location (glacier surface or bed), as well as any abiotic or biotic processing as

43 meltwater transits the glacial system. At the glacier surface, allochthonous DOM may derive
44 from the deposition of aerosols comprising fossil fuel combustion by-products^{15, 21-24} and
45 wind-blown organic material²⁵. Allochthonous DOM at the bed likely originates from
46 overridden material (ancient terrestrial origin)¹ or via inputs of DOM from the surface where
47 hydrological connections exist. Autochthonous DOM, arising from in situ microbial
48 production, is generated largely via photoautotrophic activity on the glacier surface^{5, 6} and via
49 chemoautotrophic metabolism at the glacier bed². The molecular composition of the DOM of
50 meltwaters may allow us to “fingerprint” surface-derived and subglacially-derived
51 compounds, and thus, would yield insight into the controls on the type and reactivity of DOM
52 exported from the GrIS⁴.

53

54 DOM export from glaciers and ice sheets may drive heterotrophic production in nearby
55 coastal and marine ecosystems¹. It may also influence primary production in these
56 ecosystems, via the uptake of amino acids and urea by some phytoplankton^{26, 27} or via the
57 remineralisation of DON to dissolved inorganic nitrogen (DIN)²⁶⁻²⁸. It is notable that nitrogen
58 is a primary limiting nutrient for phytoplankton productivity in many of the world’s oceans²⁹,
59 including basins surrounding the GrIS, e.g. the Labrador Sea³⁰, and the West Greenland³¹ and
60 NE Greenland coasts²⁹. Reduced levels of DIN are commonly observed in marine surface
61 waters in summer, causing a decline in primary productivity after the seasonal maxima in
62 spring^{29, 32}. Primary production also plays a critical role in the net biologically-mediated
63 exchange of CO₂ between the atmosphere and ocean³³, which exerts an important regulatory
64 effect on the global climate system³⁴. Summer nutrient limitation of phytoplankton in the
65 Arctic may be enhanced in the future as ocean temperatures increase and marine growing
66 seasons lengthen³⁵. Since nitrogen is a limiting nutrient in the Greenland fjords²⁹ and near

67 coastal oceans^{30, 36}, DON and DIN inputs from external sources such as glaciers and ice
68 sheets, are of key importance.

69

70 Here, we investigate the abundance and composition of DOM exported from Leverett
71 Glacier, a large (>600 km²) land-terminating GrIS glacier, during the 2010 melt season. We
72 focus on the presence and proportion of DOM formulas with an N-rich component and low
73 aromatic carbon content. Aliphatic DOM with low C:N ratios may be considered highly
74 bioavailable for microbial metabolism³⁷, and thus may have the potential to support
75 downstream primary productivity. ESI FT-ICR MS was used to determine the elemental
76 compositions of specific molecules within the DOM and identify compositional differences
77 among DOM pools²⁰. We assign elemental formulas solely from the mass measurement,
78 owing to the high mass accuracy (<1 ppm) of this technique^{38, 39}. We extend previous work
79 using ESI FT-ICR MS to investigate glacial systems^{20, 22} to provide the first detailed temporal
80 analysis of the molecular composition of DOM exported in GrIS runoff, and identify the key
81 controls on the export of N-rich DOM.

82

83 METHODS

84

85 **Field Site and Sample Collection.** Glacial samples were collected during the 2010 melt
86 season from Leverett Glacier, West Greenland (~67.10° N, 50.20° W). Leverett Glacier
87 drains a large catchment area (>600 km²), with an altitudinal range of 100 to >1200 m a.s.l,
88 and is representative of many large land-terminating Greenland outlet glaciers along the
89 western margin. Several re-advances over Quaternary deposits containing fresh organic
90 matter (e.g. paleosols) during the late Holocene⁴⁰ suggest a highly dynamic regional ice
91 margin. Runoff is exported through a primary subglacial channel which drains into a large

92 proglacial river system. This river system joins the Watson River, which discharges into
93 Kangerlussuaq Fjord, eventually emptying into the Davis Strait and the northern arm of the
94 Labrador Sea. Supraglacial meltwater samples were collected on July 20th (day of year (DY)
95 201) and August 11th (DY 223). A total of 12 subglacial runoff samples were collected from
96 the main outflow channel, ~2.2 km from the Leverett Glacier portal, between May and
97 August (Table S1). Water stage in the subglacial outflow channel was logged at 5 minute
98 intervals and converted to discharge using a rating curve ($r = 0.92$) with an uncertainty of \pm
99 14% (as detailed in^{41, 42}). Snowline migration at Leverett Glacier was delineated from
100 Moderate-resolution Imaging Spectrometer (MODIS)⁴³ imagery (detailed in the
101 Supplementary Methods).

102

103 **Sample Filtration and Preparation in the Field.** Glacial samples for DOC and major ion
104 analyses were collected in pre-furnaced (400 °C for 6 hrs) borosilicate glass bottles and
105 filtered <2 hrs after collection using either plastic apparatus with 0.45 μm cellulose-nitrate
106 membrane filters (major ion determination) or pre-furnaced glass filtration apparatus with
107 pre-furnaced GF/F filters (0.70 μm nominal pore size; DOC determination). Filtered water
108 samples were stored in the dark at -12 °C (in-field freezer) prior to storage in the University
109 of Bristol LOWTEX facility (≤ -20 °C). Glacial samples for mass spectrometry analysis were
110 collected in acid-cleaned polycarbonate bottles. Approximately 5 L of meltwater was
111 collected for the supraglacial samples. For the subglacial samples, 2 L was collected due to
112 higher anticipated DOC concentrations in these meltwaters. Due to the high suspended
113 sediment load, subglacial samples were first pre-filtered through 0.7 μm GF/F filters. The
114 subglacial filtrate and the supraglacial samples were then filtered through pre-furnaced 0.2
115 μm Anodisc membrane filters and acidified to pH 3 with 12 M HCl (Trace-Metal grade,
116 Thermo Fisher Scientific). Filtered water samples for mass spectrometry analysis were stored

117 in a cold, dark field environment and were refrigerated ($\sim 4\text{ }^{\circ}\text{C}$) < 7 days after collection and
118 frozen ($-20\text{ }^{\circ}\text{C}$) on return to Woods Hole Oceanographic Institution (WHOI).

119

120 **DOC Determination.** DOC, measured as non-purgeable organic carbon, was determined
121 by high temperature combustion (680°C) using a Shimadzu TOC-V_{CSN} Analyzer equipped
122 with a high sensitivity catalyst. Daily precision and accuracy determined via repeat analysis
123 of a DOC standard solution containing potassium hydrogen phthalate ($\text{C}_8\text{H}_5\text{KO}_4$) (Merck,
124 DE) were $< \pm 6\%$. The limit of detection was $5\text{ }\mu\text{M C}$.

125

126 **Major Ion Determination.** Major anions (Cl^- , NO_3^- , SO_4^{2-}) and cations (Na^+ , K^+ , Mg^{2+} ,
127 Ca^{2+}) were measured on a DX-500 Ion Chromatograph (Dionex, Sunnyvale, CA, USA).
128 HCO_3^- was calculated by charge deficit. Measurement precision and accuracy was *c.* $\pm 4\%$
129 and *c.* $\pm 7\%$, respectively, although this increased near the instrument detection limit (*c.* 0.5
130 $\mu\text{eq L}^{-1}$). SO_4^{2-} , K^+ , Na^+ , Mg^{2+} and Ca^{2+} concentrations in basal ice and subglacial runoff
131 samples were corrected for snowpack contributions⁴⁴, and the residual crustal-derived
132 component is denoted with an asterisk (*).

133

134 **Solvent Extraction.** DOM was extracted with 6 mL PPL cartridges (1 g resin, Varian). The
135 solvent extraction protocol was modified from⁴⁵. Briefly, the cartridges were pre-cleaned
136 according to the manufacturer's instructions (2 volumes of 100% MeOH, Optima grade). The
137 acidified samples were then passed through the cleaned cartridges and the cartridges rinsed
138 with 0.01 M HCl. The cartridges were dried (under a vacuum) for 5 min then the DOM was
139 eluted (by gravity) with MeOH into a pre-furnaced amber vial with PTFE-lined cap. Samples
140 were frozen and later evaporated to dryness under vacuum at $30\text{ }^{\circ}\text{C}$. A procedural blank
141 (MeOH) was also evaporated to dryness under vacuum. The samples and solvent blank were

142 stored dry at -20 °C until further analysis. The DOM extraction efficiency was likely between
143 40 and 60%⁴⁵.

144

145 **FT-MS Data Acquisition.** All samples and the solvent blank were analysed on a 7-T ESI
146 FT-ICR mass spectrometer (LTQ-FT-MS, Thermo Fischer Scientific, Waltham, MA) at the
147 WHOI mass spectrometry facility. Samples were reconstituted in 70% MeOH, and analysed
148 in negative ion mode. The solvent used to dilute the samples (70% MeOH) was also analysed
149 as an instrument blank. Samples were infused into the ESI interface at 5 $\mu\text{L min}^{-1}$, and
150 instrument parameters were optimized for each sample. Samples were diluted to optimize
151 spray conditions; dilutions ranged from 1:2 to 1:8. The capillary temperature was set at 250
152 °C, and the spray voltage varied between 3.60 and 4.10 kV. As in²⁰, ~200 scans were
153 collected for each sample. The mass range for full-scan negative ion mode collection was 100
154 $< m/z < 1000$. Weekly mass calibrations were performed with an external standard (Thermo
155 Calibration Mix), and resulted in mass accuracy errors of < 1 ppm. The target average
156 resolving power was 400,000 at m/z 400.

157

158 **FT MS Data Analysis.** Peak detection, solvent blank correction, peak calibration and
159 elemental formula assignments followed the protocol described in²⁰. Negative ion mode
160 spectra were internally re-calibrated using the m/z values provided in Table S2. After internal
161 re-calibration, the root mean square (RMS) errors for the calibrants ranged from 0.08 to 0.20
162 (mean value: 0.11). As in previous work²⁰, elemental formulas of our samples were compared
163 to those assigned to Suwannee River Fulvic Acid (SRFA) Standard I (Suwannee River –
164 International Humic Substances Society, Stock #1S101F), previously analysed with negative
165 ion mode ESI FT-ICR MS, to identify terrestrially-derived components. Similarly, Pony Lake
166 Fulvic Acid (PLFA) Reference (International Humic Substances Society, Lot #1R109F),

167 analysed in negative ion mode, was used to identify microbially-derived components of our
168 Greenland samples. Magnitude-averaged elemental ratios and double bond equivalencies
169 (DBE), a proxy for the amount of double-bonds and rings in a molecule, were also
170 calculated⁴⁶ (Table S3).

171

172 **Multivariate Statistics.** Differences among all samples in our dataset were assessed using
173 cluster analysis and non-metric multidimensional (NMS) scaling based on a Bray-Curtis
174 distance measure. For this analysis we limited our interpretation solely to peak diversity by
175 transforming all relative peak heights to presence (peak height = 1) or absence (peak height =
176 0). This was done in order to circumvent known issues associated with using peak height²⁰. In
177 the cluster analysis, Ward's linkage was used to group the samples, and p-values for each
178 cluster were calculated via multiple bootstrap resampling (see Supplementary Methods). No
179 additional information was gained from the NMS ordinations so we focus here only on the
180 cluster analysis (Figure 1). The cluster analysis separated the samples into four significantly
181 different groups: Sub1, Sub2, Sub3 and Supra. We then reduced the complexity of our dataset
182 by focusing on the peaks that appear more than once in each group. Thus, we derived what
183 we refer to as 'consolidated sample groups'. For instance, peaks present in Sub1 had to be
184 present in >1 of the samples that are included in the Sub1 group defined by the cluster
185 analysis. This increased our confidence in our observations because they are based on
186 repeatable *m/z* values, rather than on the full dataset, which may contain spurious noise peaks
187 and/or peaks near the signal-to-noise threshold. We also defined 'unique sample groups' for
188 subglacial and supraglacial samples, which required peaks to be present in either only
189 supraglacial sample groups or only subglacial sample groups (labelled 'unique supra' and
190 'unique sub' respectively). Wilcoxon rank-sum tests were conducted to assess the
191 significance of differences in magnitude-averaged N:C, H:C, DBE, and the percentages of

192 condensed hydrocarbons and terrestrial-like compounds in Supra, Sub1, Sub2 and Sub3
193 groups (see Supplementary Methods, Table S4).

194

195 RESULTS

196

197 Formulas were assigned for >90% of the resolved peaks (4999-8747 peaks) in all samples
198 in this dataset (Table S3). Between 29-45% of the peaks identified by ESI FT-ICR MS were
199 assigned to formulas containing CHO (Table 1), with small but significant contributions (18-
200 29%) from other heteroatoms such as S and P. The relative contribution of N is very high,
201 with 27-41% of formulas containing CHON. This is consistent throughout this dataset and
202 contrasts with other published freshwater and marine datasets⁴⁶⁻⁴⁸. In comparison to other
203 glacial datasets, the N-containing compounds in this study are within the range previously
204 reported from the European Alps (5-58% as determined by FT-ICR MS)¹⁵. Interestingly, this
205 N-rich component is present regardless of the glacial source, appearing in both supraglacial
206 and subglacial samples. We analyzed a SRFA standard during these sample runs to monitor
207 instrument performance and ascertained that the instrument was not biased toward N-
208 containing formulas. Therefore, we conclude that these samples are particularly N-rich in the
209 ESI-amenable component of glacial-derived DOM.

210

211 We ran a hierarchical cluster analysis and identified four clusters that are distinct at the
212 90% significance level (based on approximately unbiased (AU) p-values). The two
213 supraglacial samples clustered together (supra, AU p-value = 94%) and are statistically
214 different from the subglacial samples (Figure 1), which clustered into three statistically
215 distinct groups (Sub1, Sub2 and Sub3). Sub1 and Sub2 are the most similar and differentiated
216 by small changes in carbohydrate and lignin percentages (Table 2). Sub3 contains lower

217 proportions of condensed hydrocarbons than Sub1 and Sub2 but higher contributions in most
218 other compound classes. Notably, many of the N-rich elemental formulas in each group
219 appear in the region associated with protein-like formulas in a van Krevelen diagram (Table
220 2, Figure S1). The proportion of protein-like elemental formulas in the consolidated sample
221 groups (19.0 – 21.6%) is similar to those from a PLFA standard (23%).

222

223 The formula assignments were found to differ between the supraglacial and subglacial
224 samples. Approximately 20% of supraglacial DOM compounds are not found in subglacial
225 runoff (based on total number of formulas assigned, Table S3), and ~50% are unique to the
226 subglacial runoff. The magnitude-averaged elemental ratios suggest that the supraglacial
227 samples are also generally more aliphatic, indicated by the higher H:C and the lower DBE
228 magnitude-averaged values (significant at the 80% and 96% confidence levels, respectively,
229 Tables S3, S4). The elemental formulas in the van Krevelen diagram regions support this
230 hypothesis with higher protein- and lipid-like compounds and lower condensed hydrocarbon
231 contributions³⁹ (Tables 2, S5) in the consolidated and unique supraglacial groups. The
232 difference in condensed hydrocarbon contributions in consolidated subglacial and
233 supraglacial samples was significant at the 96% confidence level (Table S4). In contrast, the
234 subglacial samples have relatively low H:C and higher DBE magnitude-averaged values,
235 likely from increased condensed hydrocarbon and terrestrial contributions⁴⁹, including
236 compounds present in SRFA, the terrestrial end-member³⁷. While the differences between
237 subglacial and supraglacial samples outlined above were statistically significant, there may be
238 some bias in the dataset created by the larger number of subglacial samples analysed relative
239 to supraglacial samples. This was unavoidable due to the time-consuming nature of sampling
240 and the logistical complexity of sampling waters far into the GrIS interior. We acknowledge

241 this potential bias when discussing differences between the DOM compositions of subglacial
242 and supraglacial waters.

243

244 There is no apparent temporal trend in the composition of the subglacial samples analysed
245 by ESI FT-ICR MS. This compares well with previous work on DOC export from the
246 catchment⁴. Bulk DOC concentrations (7-32 $\mu\text{M C}$) were comparable to concentrations in
247 other glacial systems^{19, 20} and were not significantly associated with discharge (Table S1). We
248 compared the timing of subglacial sample acquisition with their DOM cluster patterns (Figure
249 2) to ascertain if there were specific hydrological or hydrochemical processes driving these
250 distinctions. We found no clear pattern in the timing of the three clusters in relation to the
251 trends in bulk discharge and major hydrological events (e.g. subglacial “outburst events”
252 denoted by shading in Figure 2).

253

254 We further compared DOM subglacial cluster patterns to geochemical proxies to determine
255 the extent to which subglacial water routing influenced these sample groups. The ratio of
256 divalent to monovalent (di:mono) cations is a proxy for rock:water residence time^{50, 51}, with
257 higher proportions of monovalent ions believed to reflect enhanced silicate dissolution in
258 long residence time subglacial waters (Figure S3). The di:mono cation ratio appeared to
259 correlate directly with the percent of protein-like formulas in Sub2 ($R^2 = 0.86$). No
260 correlations were observed in Sub1 and geochemical associations were not determined for
261 Sub3 due to the small sample size ($n=3$).

262

263 DISCUSSION

264

265 **Molecular character of GrIS DOM.** The detailed characterisation of DOM compounds by
266 ESI FT-ICR MS illustrates the unique character of glacial DOM. The wide distribution of
267 assigned formulas within the van Krevelen diagram, including condensed hydrocarbons,
268 lipids, lignins, proteins, carbohydrates and terrestrial groups, and the large diversity in
269 compound formulas within the groupings shows that a chemically diverse range of DOM
270 compounds is exported in runoff from the GrIS. We attribute this to the existence of multiple
271 surface and basal sources for DOM within this large ice sheet catchment, which mix to form
272 the meltwaters exported via the glacier portal at the margin. Glacially-derived DOM also
273 differs markedly to that from marine and other freshwater systems due to higher proportions
274 of N-rich elemental formulas and protein-like formulas (Tables 1, 2, S3). Our characterisation
275 of GrIS DOM is consistent with recent FT-ICR MS analyses of glacial DOM in Alaska²¹, the
276 Alps¹⁵ and Greenland²⁰, and hence, we support the notion that DOM exported from glaciers
277 and ice sheets has a unique molecular signature, albeit influenced by the degree of
278 supraglacial vs. subglacial inputs, which we consider below.

279

280 **Different compounds from the glacier surface and bed.** We performed an inter-
281 comparison of subglacial and supraglacial spectra and found some distinct contrasts in DOM
282 composition which may indicate different pathways of DOM production and transformation
283 in surface and basal environments. However, some differences may arise from the very
284 different number of samples analysed from subglacial and supraglacial environments. The
285 latter may particularly explain the significantly higher (at the 96% confidence level)
286 proportion of condensed hydrocarbons in the subglacial samples compared with the
287 supraglacial samples (Table S4). Condensed hydrocarbons are associated with the
288 combustion products found in anthropogenic aerosols²¹ and likely originate from the
289 atmospheric deposition of soot particles⁵² containing black carbon-like molecules⁵³. The

290 condensed hydrocarbons in the subglacial samples are thought to derive from the deposition
291 of anthropogenic aerosols on the glacier surface and their subsequent transport to the glacier
292 bed via moulins and surface lake drainage^{4, 41}. Supraglacial meltwater sampled in this study
293 was collected only 2 km from the GrIS margin, and contained low proportions of condensed
294 hydrocarbons (8.7%), similar to a previous study on the GrIS which reported 6.8%²⁰. Here,
295 high levels of erosion on steep ice surfaces is common and may preclude accumulation of
296 condensed hydrocarbons⁵⁴. Earlier research reports higher condensed hydrocarbon percentage
297 contributions in GrIS snow and supraglacial samples located further inland (12.6% and
298 16.0%, respectively)²⁰. The reduced physical erosion of surface particulate material in flatter,
299 inland areas of ice and snow permits the accumulation of organic matter, including condensed
300 hydrocarbons, over successive melt seasons⁵⁴. Runoff exported from Leverett Glacier is
301 predominantly sourced from such inland areas, where condensed hydrocarbon contributions
302 are known to be higher²⁰. These findings imply some degree of sample bias introduced by the
303 collection of our supraglacial samples close to the ice margin, when runoff is sourced from a
304 much wider area.

305

306 The high N:C ratios identified by ESI FT-ICR MS in the supraglacial (Table S3, mean =
307 1.47 ± 0.13) and subglacial samples (mean = 1.35 ± 0.07) suggest that nitrogen-containing
308 molecules may be a major contributor to glacial DOM⁵⁵. While supraglacial samples were
309 shown to have significantly higher N:C ratios compared with subglacial samples, we do not
310 discuss this difference due to the lower confidence levels (87%) and the potential bias
311 towards the more numerous subglacial samples. Our overall observations concur with those
312 reported in glacial systems elsewhere, which show a high proportion of N-rich formulas in
313 ice cores²², supraglacial meltwater²⁰, and runoff from an Arctic Glacier (based on high
314 percentage of protein-like fluorescence)¹. There are two possible sources of the N-rich

315 aliphatics observed in supraglacial DOM; the water-soluble organic carbon fraction in
316 aerosols^{21, 56} or *in situ* microbial activity^{15, 20}. Similarly, the provenance of the high proportion
317 of lipid-like compounds found in the supraglacial samples (mean = $1.85 \pm 0.07\%$, compared
318 with a mean of $0.81 \pm 0.21\%$ in the subglacial samples, Table S4) may also be microbial^{20, 57,}
319 ⁵⁸ or aerosol⁵⁹. The high proportion of protein-like formulas in the supra group (21.6%) may
320 also reflect a microbial origin for the N-rich DOM. Protein-like compounds have previously
321 been interpreted as evidence for *in situ* microbial activity^{13, 36, 53} and likely derive from the
322 highly productive photosynthetic microbial communities on the GrIS surface⁵⁴. Based on the
323 large proportion of protein-like compounds, we believe that *in situ* microbial production is
324 the most likely source of the N-rich DOM on the GrIS surface. This is a pertinent observation
325 since it implies high bioavailability of DOM to downstream microbial communities^{1, 4}, which
326 may include communities in the glacier subsurface¹³.

327

328 Our data also suggest that physico-chemical processes in the subglacial environment may
329 generate new DOM compounds of a distinct character that are not observed on the glacier
330 surface. The presence of unique subglacial formulas is consistent with the addition of new
331 DOM compounds as meltwaters transit the subglacial environment. Unique subglacial
332 compounds typically have high aromaticity which likely reflects the leaching of more
333 recalcitrant, terrestrial material from paleosols known to be present in the catchment⁷. The
334 significantly higher DBE values in subglacial samples compared with supraglacial samples
335 also suggests that allochthonous sources, such as overridden terrestrial material, may be a
336 major contributor to subglacial DOM beneath the GrIS. A terrestrial origin for DOM
337 produced in subglacial environments has been reported elsewhere^{19, 60}. Contact with
338 particulate organic matter on the GrIS surface is limited to windblown debris from both local
339 proglacial terrain and more distant sources, explaining the lower proportion of terrestrial-like

340 compounds in the supraglacial DOM. It is notable that only 14% of the uniquely supraglacial
341 formulas was categorized as terrestrial (Table 2) compared with 31% of the uniquely
342 subglacial formulas. We also find evidence of microbial production of DOM compounds in
343 the subglacial environment based on 18% of the protein-like compounds identified by ESI
344 FT-ICR MS being classified as unique-subglacial (Table 2). Thus a key finding is that N-rich
345 DOM may also derive from the glacier bed. These N-rich compounds may be generated by a
346 range of microbial processes such as in situ chemoautotrophic production^{2, 61},
347 chemoheterotrophic oxidation of OM substrates to lower molecular weight compounds²⁰
348 and/or the release of DOM from decaying cells. Glacially-overridden material can thus act as
349 a direct or indirect (via microbial cycling) source of DOM.

350

351 **N-rich export from Leverett Glacier throughout the melt season.** We provide the first
352 detailed temporal analysis of the molecular composition of DOM exported in glacial runoff
353 and show that N-rich DOM emerges throughout the melt season¹⁶⁻¹⁸ as the snow line retreats
354 up glacier, with no association with discharge. Mean DON concentrations (~2.3 μM) in
355 Leverett Glacier runoff sampled in 2012 accounted for >50% of the total dissolved nitrogen
356 flux¹⁸, supporting recent work that proposes glacial systems as a source of bioavailable
357 material to downstream ecosystems^{1, 2, 4}. We assert that the intermittent tapping of new
358 subglacial and surface DOM sources, including the flushing out of stored subglacial water by
359 rapid supraglacial inputs, or “outburst events”, creates the unique DOM signature in GrIS
360 runoff and provides the continuous export of N-rich DOM. This suggests that DOM export
361 from Leverett Glacier comprises inputs from multiple sources, which contribute to the net
362 export throughout the melt season. Supraglacial meltwater, containing DOM sourced from
363 snow and from supraglacial microbial activity, may be transferred rapidly through the glacier
364 system (channelized drainage). Meltwater contributions from the distributed drainage system

365 also contribute to the net DOM export. Meltwater transport rates are typically slow in this
366 latter drainage system and may include DOM derived from in situ microbial metabolism of
367 subglacial organic substrates during over winter storage⁶². The concentration and
368 composition of DOM in meltwater illustrate little change as the slow, inefficient distributed
369 drainage component is diluted by the fast, efficient channelized drainage system. This implies
370 that there is no exhaustion of specific DOM types as the melt season at Leverett Glacier
371 progresses.

372

373 The lack of seasonal exhaustion of DOM types may be explained by the large ablation zone
374 (> 600 km² during peak melt) and the potential for meltwaters to access new DOM sources at
375 the ice surface and bed in response to retreat of the snowline further inland⁴. We compare the
376 distribution of compound classes in subglacial samples from a small ('N' Glacier, ~5 km²)²⁰
377 and large (Leverett Glacier) GrIS outlet glacier to investigate whether glaciers with different
378 catchment sizes influence the DOM composition in Greenland. Key differences observable
379 between individual subglacial samples from these two glaciers for samples collected in June-
380 August are a) a higher proportion of terrestrial-like compounds in 'N' Glacier subglacial
381 runoff (56%²⁰, compared with 26-34% for Leverett Glacier, Table S5), and b) a higher
382 proportion of CHON formulas and protein-like compounds in Leverett Glacier subglacial
383 runoff (27-41% and 16-22%, respectively) compared with 'N' Glacier (8-10% for both, Table
384 1). Ice sheet surfaces can be divided into three 'ecological zones'; the marginal zone, the bare
385 ice zone and the slush zone^{54, 63}. Runoff at Leverett Glacier is dominated by melt sourced
386 from the bare ice zone, which may extend ~100 km into the GrIS interior (Figure S2). This
387 contrasts with 'N' Glacier where most of the runoff is derived from the marginal zone.
388 However, contrasts in melt zone proportional contributions to runoff may not fully explain
389 the differences in the DOM compound classes in subglacial runoff between the two glaciers.

390 Glacier margin supraglacial samples presented here and in ²⁰ show a higher % CHON and
391 protein-like content, and a lower % terrestrial contribution than those sampled from further
392 inland (presented in ²⁰). This is the reverse of what would be required to explain differences
393 in subglacial runoff from the two systems based upon contrasting runoff contributing areas.
394 This tentatively suggests that the differences in compounds classes in runoff from the two
395 glacier systems arise from processes at the GrIS bed. The GrIS margin has fluctuated
396 considerably over the last few 1000 years, resulting in the sequestration of soil carbon
397 beneath the ice sheet⁶⁴. It is likely that 'N' Glacier overrode a larger area of soil relative to
398 the total catchment size, compared with Leverett Glacier, as it is confined to the marginal
399 zone of the GrIS. This would explain the larger percentages of terrestrial-like compounds at
400 'N' Glacier and the lower percentages of CHON and protein-like formulas (when excluding
401 the 'N' Glacier May sample), which may arise from modification of the DOM composition as
402 meltwaters leach DOM from a subglacial soil layer or as N-rich glacial DOM is utilized for
403 microbial activity in this soil layer. This suggests that contrasts in DOM character between
404 glaciers in Greenland may be due to contrasts in the overridden substrate material.

405

406 At large GrIS outlet glaciers, additional solute acquisition during periods of high bulk
407 meltwater are expected to counter dilution effects normally occurring when a solute-rich
408 baseflow component is diluted by a solute-poor channelized component⁴. Here, this is
409 illustrated by the absence of an inverse association between DOM concentrations and bulk
410 meltwater discharge. The geochemical proxy employed (ratio of di:mono cations) also shows
411 that meltwater residence time in the subglacial drainage system, and the resultant character of
412 DOM in subglacial export, is more complex than the typical relationship between
413 geochemical species and residence time as applied to smaller glacier systems⁴⁴. Monovalent
414 ion concentrations are thought to increase in longer residence time waters due to enhanced

415 silicate, relative to carbonate, dissolution⁵¹, resulting in a lower di:mono ratio. Higher ratios
416 are indicative of carbonate weathering and rapid meltwater transport through the subglacial
417 system⁵⁰. In Sub2, there is evidence that the percentage of protein-like compounds increases
418 with the di:mono ratio (Figure S3), which may be indicative of a supraglacial origin and
419 rapid, conservative transport through the glacial system with limited subglacial storage at
420 times when subglacial residence time are low. However, no trends were observed in Sub1 and
421 we were unable to conduct a robust regression analysis on Sub3 due to the small sample
422 number (n=3). The lack of significant associations between these geochemical indices may
423 support earlier assertions that meltwater from a range of sources is constantly being flushed
424 through the subglacial drainage system. This is strengthened by the lack of a temporal trend
425 in the export of the subglacial groups and evidence that the net meltwater export comprises
426 runoff that is delivered through several hydrological pathways

427

428 In summary, our results indicate that the molecular composition of DOM exported from
429 large, GrIS outlet glaciers is compositionally diverse and exhibits a high proportion of N-rich
430 and protein-like formulas compared with marine and other freshwater systems. The source
431 for the protein-like compounds is likely to be microbial activity at the surface and bed of the
432 ice sheet, but we cannot rule out the possibility that there is also an aerosol source for N-
433 containing formulas. The continuous supply of this potentially highly bioavailable DOM to
434 runoff throughout the melt season implies a lack of any seasonal exhaustion trend in the study
435 year. It suggests that new sources of DOM are tapped at the surface and bed with progressive
436 retreat of the snowline. As such, the GrIS may be providing an important nitrogen subsidy to
437 proglacial, fjord and coastal marine environments, where such bioavailable DOM may be
438 particularly important in sustaining microbial production at the height of the summer melt
439 season.

440 Table 1 General parameters from negative ion mode formula assignments. Elemental ratios
 441 were calculated as magnitude-averaged values from m/z values with assigned elemental
 442 formulas. Previously published general parameters from other environments are also shown
 443 for comparison. The consolidated group name is given in parentheses for samples reported in
 444 this study. ‘n.r.’ means the data was not reported. §proglacial tarn sampled at the margins of
 445 the Greenland Ice Sheet. †Antarctica. ¹recalculated from raw data published in reference.
 446 ²mean, n=4. ³CHONS only. SRFA = Suwannee River Fulvic Acid. WSOC = Water Soluble
 447 Organic Carbon. DY = day of year.

448

Sample – Group	% formula with CHO	% formula with CHON	% formula with CHONS, CHONP, CHONSP	Reference
<i>Greenland Supraglacial</i>				
DY 201 (Supra)	31.5	31.5	26.1	This study
DY 223 (Supra)	35.2	27.0	28.6	This study
Snow	17.4	23.4	42.5	Bhatia et al., (2010)
Supra inland	1.7	32.0	50.1	Bhatia et al., (2010)
Supra margin	23.3	34.7	23.0	Bhatia et al., (2010)
<i>Greenland Subglacial</i>				
DY 178 (Sub1)	32.1	36.4	22.4	This study
DY 181 (Sub1)	32.2	35.6	23.1	This study
DY 207 (Sub1)	29.8	40.9	20.5	This study
DY 220 (Sub1)	34.7	38.9	18.6	This study
DY 151 (Sub2)	34.1	33.7	23.3	This study
DY 164 (Sub2)	38.2	33.3	21.3	This study
DY 212 (Sub2)	36.2	34.7	20.8	This study
DY 218 (Sub2)	40.1	31.7	21.5	This study

DY 224 (Sub2)	37.5	36.3	18.2	This study
DY 161 (Sub3)	29.4	39.8	23.6	This study
DY 204 (Sub3)	36.3	32.1	23.5	This study
DY 210 (Sub3)	44.5	27.4	21.6	This study
May Sub	55.6	26.1	11.3	Bhatia et al., (2010)
July Sub 1	69.2	8.1	18.9	Bhatia et al., (2010)
July Sub 2	58.9	10.8	26.2	Bhatia et al., (2010)
<i>Terrestrial End-Members</i>				
Proglacial tarn[§]	65.7	12.3	17.5	Bhatia et al., (2010)
SRFA	91.3	2.0	4.5	Bhatia et al., (2010)
<i>Microbial End-Member</i>				
Pony Lake[†]	31.2	58.4	5.1	This study
<i>Fresh Water</i>				
Delaware River¹	91.6	0.6	0.8	Kujawinski et al., (2009)
Chesapeake Bay^{2*}	90.5	Sum: 9.5%*	n.r.	Sleighter and Hatcher (2008)
<i>Surface Water</i>				
Sargasso Sea¹	78.8	6.6	2.0	Kujawinski et al., (2009)
<i>Deep Ocean</i>				
Sargasso Sea¹	72.2	2.4	5.4	Kujawinski et al., (2009)
<i>Aerosol-derived WSOC</i>				
Virginia³	77.0	12.0	<1.0	Wozniak et al., (2008)
New York³	75.0	6.0	<1.0	Wozniak et al., (2008)

449
450
451

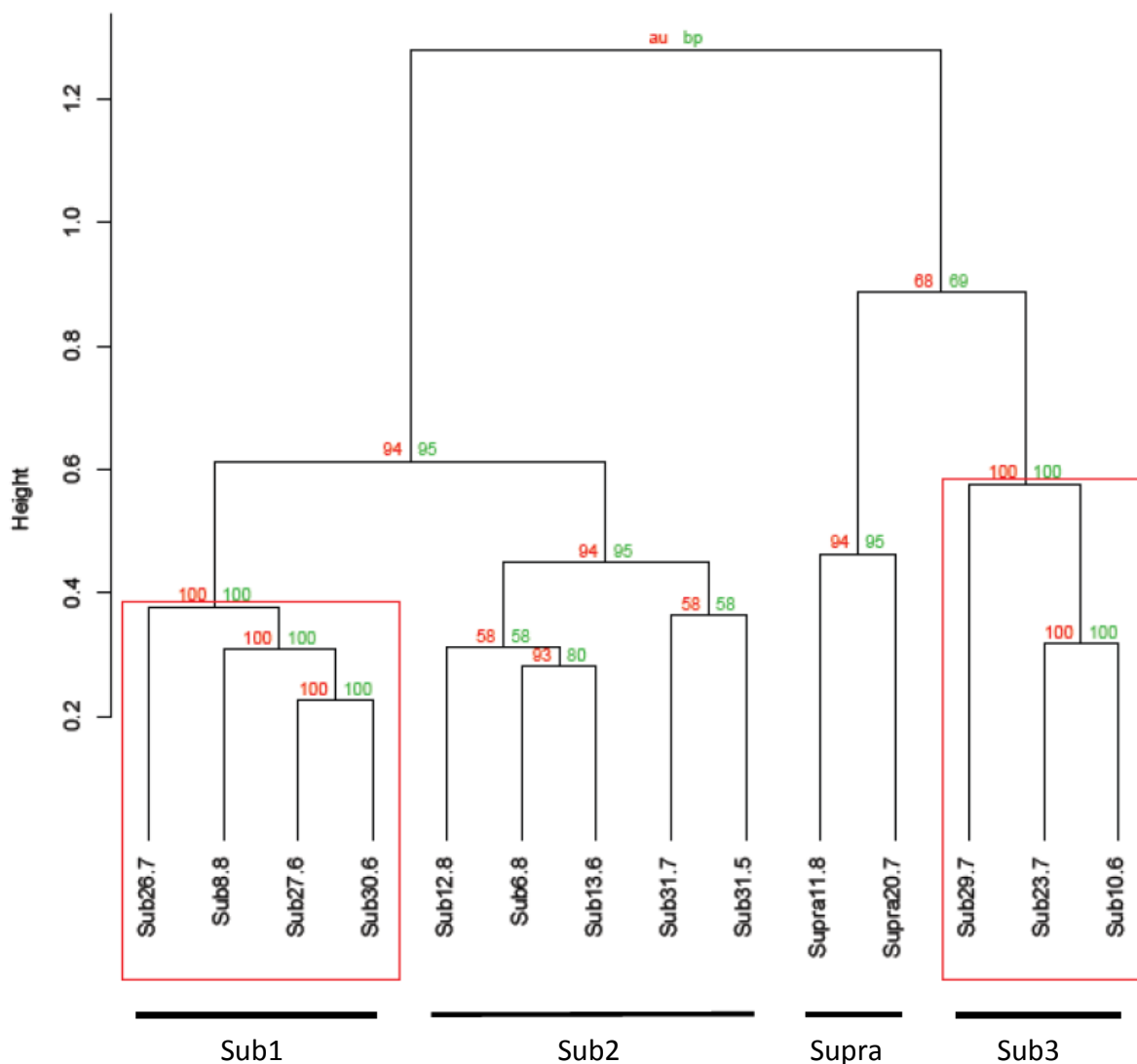
*Values from Chesapeake Bay Bridge were not reported as individual formula classes and are shown here as the sum of non-CHO formulas (as in reference).

452 Table 2. Percentage of negative ion mode formula assignments located in different regions of the van Krevelen diagram for each consolidated
 453 group, and the percentage unique to the subglacial and supraglacial groups. Data that was not reported is denoted by “n.r”. † = Antarctica. * =
 454 recalculated from raw data in Kujawinski et al., (2009). SRFA = Suwannee River Fulvic Acid. The terrestrial compound class refers to formula
 455 assignments that exactly matched the SRFA samples.

456

Sample	Condensed hydrocarbons	Lipids	Lignin	Protein	Carbohydrate	Terrestrial	Reference
Supra	8.7	1.81	5.5	21.6	0.40	21.9	This study
Sub1	11.1	0.67	6.3	20.6	0.55	29.3	This study
Sub2	11.5	0.72	5.8	19.6	0.31	30.6	This study
Sub3	9.5	0.88	6.8	19.0	0.41	30.2	This study
Unique supra	6.0	4.10	1.5	13.6	0.00	14.0	This study
Unique Sub	12.4	0.54	5.4	18.0	0.53	31.4	This study
SWFA	2.0	0.00	4.5	1.9	0.00	85.6	Bhatia et al., (2010)
Pony Lake†	3.0	0.30	10.0	23.0	0.90	45.0	This study
Fresh Water*	1.9	0.40	25.5	11.9	0.00	54.9	Kujawinski et al., (2009)
Surface Water*	9.0	0.30	21.9	12.4	0.00	57.6	Kujawinski et al., (2009)
Deep Ocean*	13.1	0.10	21.6	6.2	0.00	65.4	Kujawinski et al., (2009)

457 Figure 1 Cluster dendrogram of the negative ion mode samples, based on presence/absence data
 458 and Bray-Curtis distance measure, using Ward's linkage method, and illustrating au/bp
 459 confidence levels (%). DY refers to day of year. au = approximately unbiased p-value (given in
 460 red in the figure) and bp = bootstrap probability value (given in blue in the figure, see
 461 Supplementary Methods). Boxes are drawn around the clusters with $au \geq 95\%$.

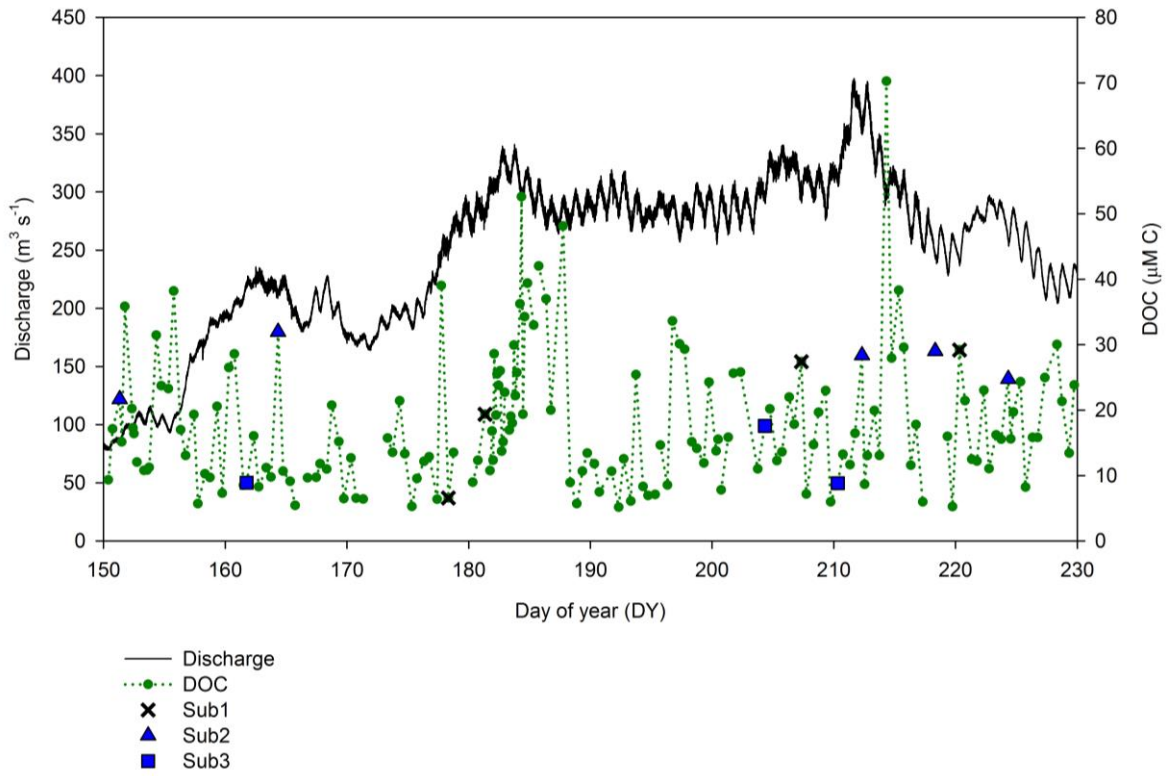


462

463 Figure 2 Time series of DOC export and discharge from Leverett Glacier including markings of
464 when subglacial samples were collected for FT-ICR MS analysis (black crosses, blue triangles
465 and squares) and outburst events (shaded).

466

467



468 ASSOCIATED CONTENT

469 Methods (delineation of the snowline and associated figure, statistical analyses (hierarchical
470 cluster analysis with p-values and Wilcoxon rank-sum test)), results tables with information on
471 sample collection, ESI FT-ICR MS and statistical analyses, a figure illustrating van Krevelen
472 diagrams for two of the samples, and a figure comparing geochemical parameters. This material
473 is available free of charge via the Internet at <http://pubs.acs.org>.

474 AUTHOR INFORMATION

475 **Corresponding Author**

476 *E. C. Lawson, Bristol Glaciology Centre, School of Geographical Sciences, University of
477 Bristol, University Road, Bristol, BS8 1SS, U.K (emily.lawson@nottingham.ac.uk)†.

478 **Present Addresses**

† School of Geography, University of Nottingham, University Park, Nottingham, NG7 2RD,
U.K.

479 **Author Contributions**

480 The manuscript was written through contributions of all authors. All authors have given approval
481 to the final version of the manuscript.

482 ACKNOWLEDGMENT

483 This research was funded by the Natural Environment Research Council UK (NERC) grant
484 NE/E004016/1 (to J. L. Wadham) and a NERC CASE studentship to E. C. Lawson (NERC
485 DTG/GEOG SN1316.6525) co-sponsored by Dionex Corporation (part of Thermo Fisher
486 Scientific). Support to J. L. Wadham was also provided by the Leverhulme Trust via a Phillip

487 Leverhulme award and a Leverhulme Trust Research Fellowship. Support to M. P. Bhatia and E.
488 B. Kujawinski was provided by a WHOI Clark Arctic Research Initiative Grant. We
489 acknowledge M. Kido Soule for assistance with data collection.

490

491 REFERENCES

492 1. Hood, E.; Fellman, J.; Spencer, R.; Hernes, P.; Edwards, R.; D'Amore, D.; Scott, D.,
493 Glaciers as a source of ancient and labile organic matter to the marine environment. *Nature*
494 **2009**, *462*, (7276), 1044-1047, DOI 10.1038/nature08580.

495 2. Bhatia, M. P.; Das, S. B.; Xu, L.; Charette, M. A.; Wadham, J. L.; Kujawinski, E. B.,
496 Organic carbon export from the Greenland ice sheet. *Geochimica et Cosmochimica Acta* **2013**,
497 *109*, 329–344, DOI 10.1016/j.gca.2013.02.006.

498 3. Bhatia, M. P.; Kujawinski, E. B.; Das, S. B.; Breier, C. F.; Henderson, P. B.; Charette, M.
499 A., Greenland meltwater as a significant and potentially bioavailable source of iron to the ocean.
500 *Nature Geoscience* **2013**, *6*, 274–278, DOI 10.1038/ngeo1746.

501 4. Lawson, E.; Wadham, J.; Tranter, M.; Stibal, M.; Lis, G.; Butler, C.; Laybourn-Parry, J.;
502 Nienow, P.; Chandler, D.; Dewsbury, P., Greenland Ice Sheet exports labile organic carbon to
503 the Arctic oceans. *Biogeosciences* **2013**, *11*, 4015-4028, DOI 10.5194/bg-11-4015-2014.

504 5. Anesio, A. M.; Hodson, A. J.; Fritz, A.; Psenner, R.; Sattler, B., High microbial activity
505 on glaciers: importance to the global carbon cycle. *Global Change Biology* **2009**, *15*, (4), 955-
506 960, DOI 10.1111/j.1365-2486.2008.01758.x.

- 507 6. Telling, J.; Stibal, M.; Anesio, A.; Tranter, M.; Nias, I.; Cook, J.; Bellas, C.; Lis, G.;
508 Wadham, J.; Sole, A., Microbial nitrogen cycling on the Greenland Ice Sheet. *Biogeosciences*
509 **2012**, *9*, (7), 2431-2442, DOI 10.5194/bg-9-2431-2012.
- 510 7. Stibal, M.; Wadham, J. L.; Lis, G. P.; Telling, J.; Pancost, R. D.; Dubnick, A.; Sharp, M.
511 J.; Lawson, E. C.; Butler, C. E. H.; Hasan, F., Methanogenic potential of Arctic and Antarctic
512 subglacial environments with contrasting organic carbon sources. *Global Change Biology* **2012**,
513 *18*, 3332–3345, DOI 10.1111/j.1365-2486.2012.02763.x.
- 514 8. Hamilton, T. L.; Peters, J. W.; Skidmore, M. L.; Boyd, E. S., Molecular evidence for an
515 active endogenous microbiome beneath glacial ice. *The ISME journal* **2013**, *7*, 1402-1412, DOI
516 10.1038/ismej.2013.31.
- 517 9. Bamber, J.; van den Broeke, M.; Ettema, J.; Lenaerts, J.; Rignot, E., Recent large
518 increases in freshwater fluxes from Greenland into the North Atlantic. *Geophys Res Lett* **2012**,
519 *39*, DOI 10.1029/2012GL052552.
- 520 10. Rysgaard, S.; Vang, T.; Stjernholm, M.; Rasmussen, B.; Windelin, A.; Kiilsholm, S.,
521 Physical conditions, carbon transport, and climate change impacts in a northeast Greenland
522 Fjord. *Arctic, Antarctic, and Alpine Research* **2003**, *35*, (3), 301-312, DOI 10.1657/1523-
523 0430(2003)035[0301:PCCTAC]2.0.CO;2.
- 524 11. Statham, P. J.; Skidmore, M.; Tranter, M., Inputs of glacially derived dissolved and
525 colloidal iron to the coastal ocean and implications for primary productivity. *Global*
526 *Biogeochemical Cycles* **2008**, *22*, (3), GB3013, DOI 10.1029/2007GB003106.

527

- 528 12. Ortega-Retuerta, E.; Jeffrey, W.; Ghiglione, J.; Joux, F., Evidence of heterotrophic
529 prokaryotic activity limitation by nitrogen in the Western Arctic Ocean during summer. *Polar*
530 *biology* **2012**, *35*, (5), 785-794, DOI 10.1007/s00300-011-1109-8.
- 531 13. Hawkings, J. R.; Wadham, J. L.; Tranter, M.; Raiswell, R.; Benning, L. G.; Statham, P.
532 J.; Tedstone, A.; Nienow, P.; Lee, K.; Telling, J., Ice sheets as a significant source of highly
533 reactive nanoparticulate iron to the oceans. *Nature Communications* **2014**, *5*, 1-8, DOI:
534 10.1038/ncomms4929.
- 535 14. Barker, J. D.; Sharp, M.; Turner, R. J., Using synchronous fluorescence spectroscopy and
536 principal component analysis to monitor dissolved organic matter dynamics in a glacier system.
537 *Hydrological Processes* **2009**, *23*, 1487-1500, DOI 10.1002/hyp.7274.
- 538 15. Singer, G. A.; Fasching, C.; Wilhelm, L.; Niggemann, J.; Steier, P.; Dittmar, T.; Battin,
539 T. J., Biogeochemically diverse organic matter in Alpine glaciers and its downstream fate.
540 *Nature Geoscience* **2012**, *5*, 110-114, DOI 10.1038/ngeo1581.
- 541 16. Hood, E.; Scott, D., Riverine organic matter and nutrients in southeast Alaska affected by
542 glacial coverage. *Nature Geoscience* **2008**, *1*, (9), 583-587, DOI 10.1038/Ngeo280.
- 543 17. Hodson, A.; Mumford, P.; Kohler, J.; Wynn, P., The High Arctic glacial ecosystem: new
544 insights from nutrient budgets. *Biogeochemistry* **2005**, *72*, (2), 233-256, DOI 10.1007/s10533-
545 004-0362-0.
- 546 18. Wadham, J.; Hawkings, J.; Telling, J.; Chandler, D.; Alcock, J.; Lawson, E.; Monteiro,
547 F.; Bagshaw, E.; Tranter, M.; Tedstone, A.; Nienow, P.; Mikkelsen, A., Glacial sediments drive

548 high nitrogen fluxes from the Greenland Ice Sheet. *Earth and Planetary Science Letters* **in**
549 **review**.

550 19. Barker, J. D.; Sharp, M. J.; Fitzsimons, S. J.; Turner, R. J., Abundance and dynamics of
551 dissolved organic carbon in glacier systems. *Arctic Antarctic and Alpine Research* **2006**, *38*, (2),
552 163-172, DOI 10.1657/1523-0430(2006)38[163:AADODO]2.0.CO;2.

553 20. Bhatia, M.; Das, S.; Longnecker, K.; Charette, M.; Kujawinski, E., Molecular
554 characterization of dissolved organic matter associated with the Greenland ice sheet. *Geochimica*
555 *Et Cosmochimica Acta* **2010**, *74*, (13), 3768–3784, DOI 10.1016/j.gca.2010.03.035.

556 21. Stubbins, A.; Hood, E.; Raymond, P. A.; Aiken, G. R.; Sleighter, R. L.; Hernes, P. J.;
557 Butman, D.; Hatcher, P. G.; Striegl, R. G.; Schuster, P., Anthropogenic aerosols as a source of
558 ancient dissolved organic matter in glaciers. *Nature Geoscience* **2012**, *5*, 198–201, DOI
559 10.1038/ngeo1403.

560 22. Grannas, A. M.; Hockaday, W. C.; Hatcher, P. G.; Thompson, L. G.; Mosley-Thompson,
561 E., New revelations on the nature of organic matter in ice cores. *Journal of Geophysical*
562 *Research-Atmospheres* **2006**, *111*, D04304, DOI 10.1029/2005JD006251.

563 23. Spencer, R. G.; Vermilyea, A.; Fellman, J.; Raymond, P.; Stubbins, A.; Scott, D.; Hood,
564 E., Seasonal variability of organic matter composition in an Alaskan glacier outflow: insights
565 into glacier carbon sources. *Environmental Research Letters* **2014**, *9*, (5), 055005, DOI
566 10.1088/1748-9326/9/5/055005.

567 24. Jenk, T. M.; Szidat, S.; Schwikowski, M.; Gäggeler, H.; Brüttsch, S.; Wacker, L.; Synal,
568 H.-A.; Saurer, M., Radiocarbon analysis in an Alpine ice core: record of anthropogenic and

569 biogenic contributions to carbonaceous aerosols in the past (1650–1940). *Atmospheric Chemistry*
570 *and Physics* **2006**, *6*, (12), 5381-5390, DOI 10.5194/acp-6-5381-2006.

571 25. Stibal, M.; Tranter, M.; Benning, L. G.; Rehak, J., Microbial primary production on an
572 Arctic glacier is insignificant in comparison with allochthonous organic carbon input.
573 *Environmental Microbiology* **2008**, *10*, (8), 2172-2178, DOI 10.1111/j.1462-2920.2008.01620.x.

574 26. Berman, T.; Bronk, D. A., Dissolved organic nitrogen: a dynamic participant in aquatic
575 ecosystems. *Aquatic Microbial Ecology* **2003**, *31*, (3), 279-305.

576 27. Zehr, J. P.; Ward, B. B., Nitrogen cycling in the ocean: new perspectives on processes
577 and paradigms. *Applied and Environmental Microbiology* **2002**, *68*, (3), 1015-1024, DOI
578 10.1128/AEM.68.3.1015-1024.

579 28. Tupas, L. M.; Koike, I.; Karl, D. M.; Holm-Hansen, O., Nitrogen metabolism by
580 heterotrophic bacterial assemblages in Antarctic coastal waters. *Polar Biology* **1994**, *14*, (3),
581 195-204, DOI 10.1007/BF00240524.

582 29. Rysgaard, S.; Nielsen, T. G.; Hansen, B. W., Seasonal variation in nutrients, pelagic
583 primary production and grazing in a high-Arctic coastal marine ecosystem, Young Sound,
584 Northeast Greenland. *Marine Ecology Progress Series* **1999**, *179*, 13-25.

585 30. Harrison, W. G.; Li, W. K. W., Phytoplankton growth and regulation in the Labrador Sea:
586 light and nutrient limitation. *Journal of Northwest Atlantic Fisheries Science* **2007**, *39*, 71-82,
587 DOI 10.2960/J.v39.m592.

- 588 31. Nielsen, T. G.; Hansen, B. W., Plankton community structure and carbon cycling on the
589 western coast of Greenland during the stratified summer situation. I. Hydrography,
590 phytoplankton and bacterioplankton. *Aquat Microb Ecol* **1999**, *16*, (3), 205-216.
- 591 32. Kattner, G.; Becker, H., Nutrients and organic nitrogenous compounds in the marginal
592 ice zone of the Fram Strait. *Journal of Marine Systems* **1991**, *2*, (3), 385-394, DOI
593 10.1016/0924-7963(91)90043-T.
- 594 33. Falkowski, P. G., Evolution of the nitrogen cycle and its influence on the biological
595 sequestration of CO₂ in the ocean. *Nature* **1997**, *387*, (6630), 272-275.
- 596 34. Gruber, N.; Galloway, J. N., An Earth-system perspective of the global nitrogen cycle.
597 *Nature* **2008**, *451*, (7176), 293-296, DOI 10.1038/nature06592.
- 598 35. Arrigo, K. R.; van Dijken, G.; Pabi, S., Impact of a shrinking Arctic ice cover on marine
599 primary production. *Geophysical Research Letters* **2008**, *35*, (19), L19603, DOI
600 10.1029/2008GL035028.
- 601 36. Smith, W. O., Primary productivity and new production in the Northeast Water
602 (Greenland) Polynya during summer 1992. *Journal of Geophysical Research: Oceans (1978–*
603 *2012)* **1995**, *100*, (C3), 4357-4370, DOI 10.1029/94JC02764.
- 604 37. McKnight, D. M.; Boyer, E. W.; Westerhoff, P. K.; Doran, P. T.; Kulbe, T.; Andersen, D.
605 T., Spectrofluorometric characterization of dissolved organic matter for indication of precursor
606 organic material and aromaticity. *Limnology and Oceanography* **2001**, *46*, (1), 38-48.
- 607 38. Kim, S.; Rodgers, R.; Marshall, A., Truly "exact" mass: Elemental composition can be
608 determined uniquely from molecular mass measurement at similar to 0.1 mDa accuracy for

609 molecules up to similar to 500 Da. *Int. J. Mass Spectrom* **2006**, *251*, 260–265, DOI
610 10.1016/j.ijms.2006.02.001.

611 39. Kujawinski, E. B.; Behn, M. D., Automated analysis of electrospray ionization Fourier
612 transform ion cyclotron resonance mass spectra of natural organic matter. *Analytical Chemistry*
613 **2006**, *78*, (13), 4363-4373, DOI 10.1021/ac0600306.

614 40. Ten Brink, N. W.; Weidick, A., Greenland ice sheet history since the last glaciation.
615 *Quaternary Research* **1974**, *4*, (4), 429-440, DOI 10.1016/0033-5894(74)90038-6.

616 41. Bartholomew, I.; Nienow, P.; Sole, A.; Mair, D.; Cowton, T.; Palmer, S.; Wadham, J.,
617 Supraglacial forcing of subglacial drainage in the ablation zone of the Greenland ice sheet.
618 *Geophysical Research Letters* **2011**, *38*, (8), L08502, DOI 10.1029/2011GL047063.

619 42. Cowton, T.; Nienow, P.; Bartholomew, I.; Sole, A.; Mair, D., Rapid erosion beneath the
620 Greenland ice sheet. *Geology* **2012**, *40*, (4), 343-346, DOI 10.1130/G32687.1.

621 43. Ardanuy, P. E.; Han, D.; Salomonson, V. V., The moderate resolution imaging
622 spectrometer (MODIS) science and data system requirements. *Geoscience and Remote Sensing*,
623 *IEEE Transactions on* **1991**, *29*, (1), 75-88, DOI 10.1109/36.103295.

624 44. Wadham, J. L.; Hodson, A. J.; Tranter, M.; Dowdeswell, J. A., The hydrochemistry of
625 meltwaters draining a polythermal-based, high Arctic glacier, south Svalbard: I. The ablation
626 season. *Hydrological Processes* **1998**, *12*, (12), 1825-1849, DOI 10.1002/(SICI)1099-
627 1085(19981015)12:12<1825::AID-HYP669>3.0.CO;2-R.

- 628 45. Dittmar, T.; Koch, B.; Hertkorn, N.; Kattner, G., A simple and efficient method for the
629 solid-phase extraction of dissolved organic matter (SPE-DOM) from seawater. *Limnol.*
630 *Oceanogr. Methods* **2008**, *6*, 230-235.
- 631 46. Sleighter, R. L.; Hatcher, P. G., Molecular characterization of dissolved organic matter
632 (DOM) along a river to ocean transect of the lower Chesapeake Bay by ultrahigh resolution
633 electrospray ionization Fourier transform ion cyclotron resonance mass spectrometry. *Marine*
634 *Chemistry* **2008**, *110*, (3-4), 140-152, DOI 10.1016/j.marchem.2008.04.008.
- 635 47. Kujawinski, E. B.; Longnecker, K.; Blough, N. V.; Vecchio, R. D.; Finlay, L.; Kitner, J.
636 B.; Giovannoni, S. J., Identification of possible source markers in marine dissolved organic
637 matter using ultrahigh resolution mass spectrometry. *Geochimica Et Cosmochimica Acta* **2009**,
638 *73*, (15), 4384-4399, DOI 10.1016/j.gca.2009.04.033.
- 639 48. Koch, B. P.; Ludwichowski, K. U.; Kattner, G.; Dittmar, T.; Witt, M., Advanced
640 characterization of marine dissolved organic matter by combining reversed-phase liquid
641 chromatography and FT-ICR-MS. *Marine Chemistry* **2008**, *111*, (3-4), 233-241, DOI
642 10.1016/j.marchem.2008.05.008.
- 643 49. Kim, S.; Kramer, R. W.; Hatcher, P. G., Graphical method for analysis of ultrahigh-
644 resolution broadband mass spectra of natural organic matter, the van Krevelen diagram.
645 *Analytical Chemistry* **2003**, *75*, (20), 5336-5344, DOI 10.1021/ac034415p.
- 646 50. Tranter, M.; Sharp, M. J.; Lamb, H. R.; Brown, G. H.; Hubbard, B. P.; Willis, I. C.,
647 Geochemical weathering at the bed of Haut Glacier d'Arolla, Switzerland - a new model.
648 *Hydrological Processes* **2002**, *16*, (5), 959-993, DOI 10.1002/hyp.309.

- 649 51. Wadham, J. L.; Tranter, M.; Skidmore, M.; Hodson, A. J.; Prisco, J.; Lyons, W. B.;
650 Sharp, M.; Wynn, P.; Jackson, M., Biogeochemical weathering under ice: Size matters. *Global*
651 *Biogeochemical Cycles* **2010**, *24*, (3), GB3025, DOI 10.1029/2009GB003688.
- 652 52. Slater, J.; Currie, L.; Dibb, J.; Benner, B., Distinguishing the relative contribution of
653 fossil fuel and biomass combustion aerosols deposited at Summit, Greenland through isotopic
654 and molecular characterization of insoluble carbon. *Atmospheric Environment* **2002**, *36*, (28),
655 4463-4477, DOI 10.1016/S1352-2310(02)00402-8.
- 656 53. Kim, S.; Kaplan, L. A.; Benner, R.; Hatcher, P. G., Hydrogen-deficient molecules in
657 natural riverine water samples—evidence for the existence of black carbon in DOM. *Marine*
658 *Chemistry* **2004**, *92*, (1–4), 225-234, DOI 10.1016/j.marchem.2004.06.042.
- 659 54. Stibal, M.; Telling, J.; Cook, J.; Mak, K. M.; Hodson, A.; Anesio, A. M., Environmental
660 controls on microbial abundance and activity on the Greenland ice sheet: a multivariate analysis
661 approach. *Microbial ecology* **2012**, *63*, (1), 74-84, DOI 10.1007/s00248-011-9935-3.
- 662 55. Reemtsma, T.; These, A.; Linscheid, M.; Leenheer, J.; Spitzzy, A., Molecular and
663 structural characterization of dissolved organic matter from the deep ocean by FTICR-MS,
664 including hydrophilic nitrogenous organic molecules. *Environmental science & technology* **2008**,
665 *42*, (5), 1430-1437, DOI 10.1021/es7021413.
- 666 56. Wozniak, A.; Bauer, J.; Sleighter, R.; Dickhut, R.; Hatcher, P., Technical Note:
667 Molecular characterization of aerosol-derived water soluble organic carbon using ultrahigh
668 resolution electrospray ionization Fourier transform ion cyclotron resonance mass spectrometry.
669 *Atmospheric Chemistry and Physics* **2008**, *8*, (17), 5099-5111, DOI 10.5194/acp-8-5099-2008.

- 670 57. Antony, R.; Grannas, A. M.; Willoughby, A. S.; Sleighter, R. L.; Thamban, M.; Hatcher,
671 P. G., Origin and sources of dissolved organic matter in snow on the East Antarctic ice sheet.
672 *Environmental science & technology* **2014**, *48*, (11), 6151-6159, DOI 10.1021/es405246a.
- 673 58. Grannas, A.; Shepson, P.; Filley, T., Photochemistry and nature of organic matter in
674 Arctic and Antarctic snow. *Global biogeochem. Cycles* **2004**, *18*, (1), GB1006, DOI
675 10.1029/2003GB002133.
- 676 59. Kawamura, K.; Seméré, R.; Imai, Y.; Fujii, Y.; Hayashi, M., Water soluble dicarboxylic
677 acids and related compounds in Antarctic aerosols. *Journal of Geophysical Research:*
678 *Atmospheres (1984–2012)* **1996**, *101*, (D13), 18721-18728.
- 679 60. Sharp, M.; Parkes, J.; Cragg, B.; Fairchild, I. J.; Lamb, H.; Tranter, M., Widespread
680 bacterial populations at glacier beds and their relationship to rock weathering and carbon cycling.
681 *Geology* **1999**, *27*, (2), 107-110, 10.1130/0091-7613(1999)027<0107:WBPAGB>2.3.CO;2.
- 682 61. Bhatia, M.; Sharp, M.; Foght, J., Distinct bacterial communities exist beneath a high
683 arctic polythermal glacier. *Applied and Environmental Microbiology* **2006**, *72*, (9), 5838-5845,
684 DOI 10.1128/AEM.00595-06.
- 685 62. Tranter, M.; Skidmore, M.; Wadham, J., Hydrological controls on microbial communities
686 in subglacial environments. *Hydrological Processes* **2005**, *19*, (4), 995-998, DOI
687 10.1002/hyp.5854.
- 688 63. Hodson, A.; Boggild, C.; Hanna, E.; Huybrechts, P.; Langford, H.; Cameron, K.;
689 Houldsworth, A., The cryoconite ecosystem on the Greenland ice sheet. *Annals of Glaciology*
690 **2010**, *51*, (56), 123-129, DOI 10.3189/172756411795931985.

691 64. Knight, P.; Waller, R.; Patterson, C.; Jones, A.; Robinson, Z., Discharge of debris from
692 ice at the margin of the Greenland ice sheet. *Journal of Glaciology* **2002**, *48*, (161), 192-198,
693 DOI 10.3189/172756502781831359.